Effectiveness of quantitative bone SPECT/CT for bone metastasis diagnosis

Takashi Ikeda[1] **BS,**
Kazuhiro Kitajima[2] **MD,**
Tatsuya Tsuchitani[1] **BS,**
Yoshiyuki Takahashi[1] **BS,**
Yasuhiko Hama[1] **BS,**
Noriko Kotura[1] **BS**

1.Department of Radiology, Hyogo College of Medicine, Hyogo, Japan, 2. Department of Radiological Technology, Hyogo College of Medicine College Hospital, Hyogo, Japan

Keywords: Bone metastasis - Bone scintigraphy - Quantitative SPECT/CT - SUV

Corresponding author:
Kazuhiro Kitajima MD, Department of Radiology, Hyogo College of Medicine, Nishinomiya, Hyogo, Japan
1-1 Mukogawa-cho, Nishinomiya, Hyogo 663-8501 Japan
Phone: +81-798-45-6883,
Fax: +81-798-45-6262
kazu10041976@yahoo.co.jp

Received:
6 August 2022
Accepted revised:
23 November 2022

Abstract

Objective: This study was conducted to investigate the utility of standardized uptake value (SUV) derived from bone single photon emission tomography/computed tomography (SPECT/CT) for diagnosing bone metastasis. **Subjects and Methods:** One hundred forty-seven patients with malignant cancer (breast or prostate cancer), joint disorders, primary skeletal disease, or cartilaginous bone neoplasms who underwent skeletal quantitative SPECT/CT were retrospectively investigated. Acquired data were classified as normal fourth lumbar vertebra, skeletal degenerative changes, or bone metastasis. Receiver operating characteristic (ROC) curves were used to determine the optimum cut-off value for SUVmax to distinguish among these diagnoses. **Results:** Mean SUVmax values for the normal L4 bone (n=101), skeletal degenerative changes (n=47) and bone metastasis (n=64) groups were 4.47±1.66 (range 1.01-11.25), 6.99±2.58 (2.21-14.6), and 25.4±15.7 (3.88-98.87), respectively. Compared to the other two groups, SUVmax for the bone metastasis group was significantly higher (P<0.001). In the normal bone group, sensitivity, specificity and accuracy for discriminating bone metastasis were 96.3%, 95.1%, and 95.7% respectively, with a best SUVmax cut-off value of 7.40. For the skeletal degenerative changes group sensitivity, specificity and accuracy were 87.5%, 93.6%, and 90.4% respectively, with a best SUVmax cut-off value of 11.26. **Conclusion:** Quantitative bone SPECT/CT may be useful for bone metastasis diagnosis.

Hell J Nucl Med 2022; 25(3): 253-259 *Epub ahead of print: 14 December 2022* *Published online: 30 December 2022*

Introduction

Osteoblastic activity can be evaluated using radionuclide bone scintigraphy with technetium-99m-methylene diphosphonate (^{99m}Tc-MDP), a widely used technique for assessment disease extent and treatment response in osteoblastic bone metastasis patients. For characterizing bone metastasis, bone scintigraphy has a high sensitivity but relatively low specificity, as benign conditions such as fracture, osteoarthritis, degenerative joint and disk diseases, can trigger increased bone turnover and radiotracer accumulation. However, three-dimensional data acquired during bone scintigraphy, termed single-photon emission computed tomography (SPECT), can be joined with those obtained with computed tomography (CT), a morphological imaging modality. Combined SPECT/CT is well known to increase the specificity of bone scintigraphy, as sites with increased ^{99m}Tc-MDP uptake can be correlated to morphological changes shown by CT imaging [1]. Moreover, recent advances have allowed for integration of CT for attenuation correction together with a sophisticated reconstruction technique, thus providing quantitative measurements with SPECT/CT suitable for standardized uptake value (SUV) calculation [2-4]. Several groups have reported clinical applications of quantitative bone SPECT/CT parameters as well as positron emission tomography (PET) for management of malignant bony disease [5-11]. Quantitative SPECT/CT may soon have an enormous effect as an imaging biomarker in modern nuclear medicine, as well as in clinical practice.

The present study was conducted to investigate the utility of SUV derived from quantitative bone SPECT/CT for discrimination of bone metastasis from skeletal degenerative changes and normal bone.

Subjects and Methods

Patients

The Ethics Committee of Hyogo College of Medicine approved the present retrospec-

tive study (number 3144) and waived the requirement for patient-informed consent. Bone scans from 147 patients (65 males, 82 females, mean 65.0±15.2 years old) including 128 with malignant neoplasms (breast cancer 76, prostate cancer 52), 9 with joint disorders, 7 with primary skeletal disease and 3 with cartilaginous bone neoplasms, referred for ^{99m}Tc-MDP bone scintigraphy examinations between April 2018 and March 2019, were retrospectively analyzed. Patient characteristics are presented in Table 1. From a review of records, patient data, including body mass index (BMI), administered ^{99m}Tc-MDP activity and time period between radiotracer injection and image acquisition, were retrieved.

Table 1. *Patient characteristics.*

Diagnosis	Number
Cancer	
Breast cancer	76
Prostate cancer	52
Joint disorders	
Pustuloticarthro-osteitis	6
Arthritis associated with inflammatory bowel disease	2
Ankylosing spondylitis	1
Primary bone disease	
Osteoid osteoma	2
Osteofibrous dysplasia	2
Bone giant cell tumor	1
Osteosarcom	1
Paget disease	1
Cartilaginous bone neoplasms	
Enchondroma	2
Chondrosarcoma	1
Total	**147**

Bone scintigraphy

At three to four hours after intravenous administration of a 555mL dose of ^{99m}Tc-MDP (FUJIFILM RI Pharma, Co., Ltd., Tokyo, Japan) or ^{99m}Tc-hydroxymethylene diphosphonate (^{99m}Tc-HMDP) (Nihon Medi-Physics Co., Ltd, Tokyo, Japan), planar bone scintigraphy was performed using a SPECT/CT scanner (NM/CT670; GE Healthcare, Pittsburgh, Pa) equipped with a low-energy high-resolution collimator. To acquire quantitative SPECT/CT images, a hybrid system was used. CT imaging was initially performed using the following parameters: tube voltage, 120kV; tube current, 40-80mA with "automA; GE Healthcare" function and noise level of 35; X-rays collimation, 20mm (16×1.25mm); table speed, 55mm/second; table feed, 27.5mm per rotation; tube rotation time, 0.5 seconds; pitch, 1.375:1; and matrix, 512×512. Computed tomography images thus obtained were reconstructed into 3.75-mm thick sections using an adaptive statistical iterative reconstruction algorithm (ASiR; GE Healthcare). Next, SPECT images were acquired with an energy peak of 140KeV with a 10% window (126-154KeV) and step-and-shot mode acquisition (15 seconds per step, 60 steps per detector) with a 3° angular increment, and body contour scanning option selected. For scatter correction, an extra window was set at 120KeV with a 5% window (114-126KeV). For SPECT, images were reconstructed using an iterative ordered subset expectation maximization algorithm (10 iterations, 10 subsets) with CT-based attenuation correction, scatter correction, and resolution recovery using the software package provided by the vendor (Volumetrix MI; GE Healthcare). A post-reconstruction filter was also applied (Gauss filter; frequency of 0.48, order of 10). After reconstruction, images were set on a 128×128 matrix, with a 4.42-mm section thickness and 1.0 zoom factor.

Image analysis

A single experienced physician certified by both a board of nuclear medicine and board of diagnostic radiology diagnosed skeletal lesions using a hybrid SPECT/CT images. The bone scan findings were compared with clinical follow-up results obtained every three to six months for one year after imaging, based on the consensus of the treating physicians. Clinical follow-up data included clinical examination findings, medical reports and imaging results. Hyperdense sites in CT images showing degenerative changes were considered to indicate skeletal degenerative disease, such as osteophytes, degenerative intervertebral joint disease, degenerative tear in the marginal area of the vertebral body, or vertebral compression without sclerotic metastasis. Then, bone metastases were identified in locations with demarcated sclerotic bone metastasis or areas that could not be explained by the presence of degenerative changes. Finally, the fourth lumbar (L4) vertebra showing no metastatic or osteoarthritic lesions visible on SPECT or CT was defined as normal bone.

A commercially available software package (GI-BONE, Aze Co., Ltd., Tokyo, Japan), which provides statistics for maximum SUV (SUVmax) [8-10], was used to analyze the bone SPECT/CT scans. The maximum concentration in the target lesion (maximum radioactivity/voxel volume)/(injected radioactivity/body weight) was used to calculate SUVmax. Maximum SUV values for all bone metastases visible on SPECT and CT findings of patients in the bone metastasis group were determined (Figure1). For the control group, SUVmax was determined for skeletal degenerative changes

shown by SPECT/CT (Figure 2). The SUVmax of the L4 vertebra was determined in a 4-5cm^3 region of interest (ROI), with no visible metastatic or skeletal degenerative lesion in SPECT or CT images (Figure 3).

Figure 1. Osteoblastic bone metastasis of the Th7 in a 68-year-old male prostate cancer patient, showing a high SUVmax of 21.3.

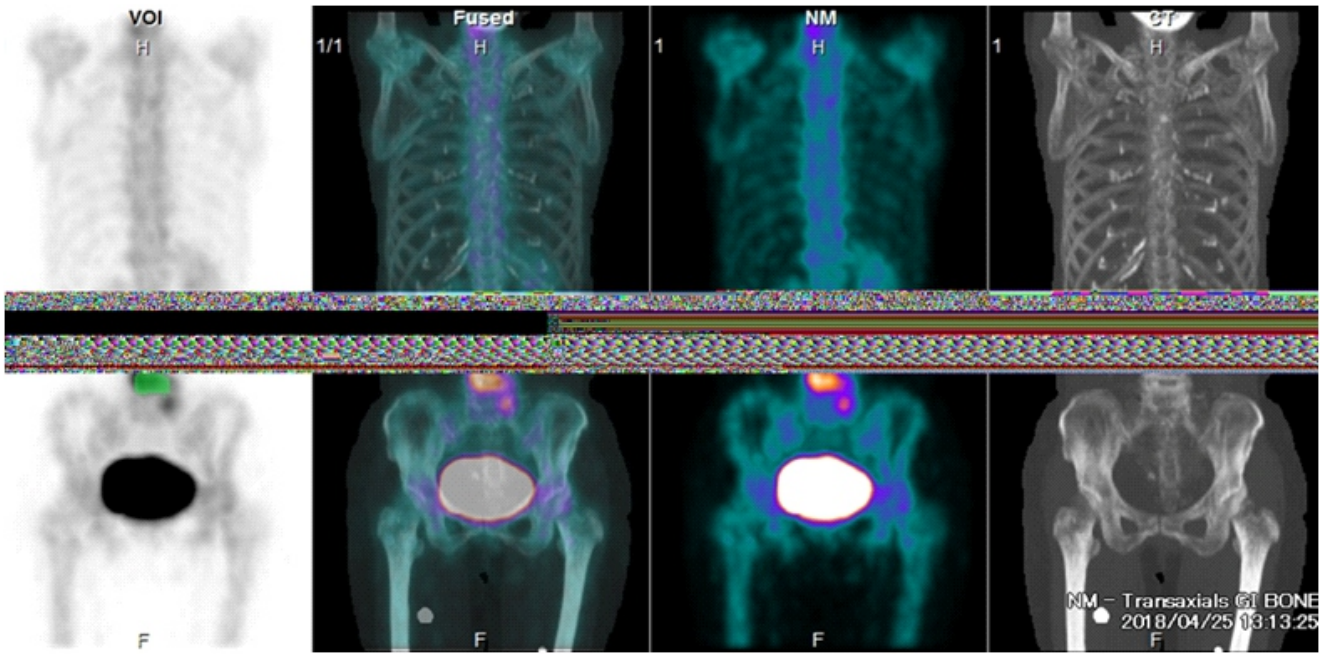

Figure 2. Osteophyte and intervertebral space of the lumber spine in a 70-year-old female breast cancer patient, showing a moderate SUVmax of 7.75.

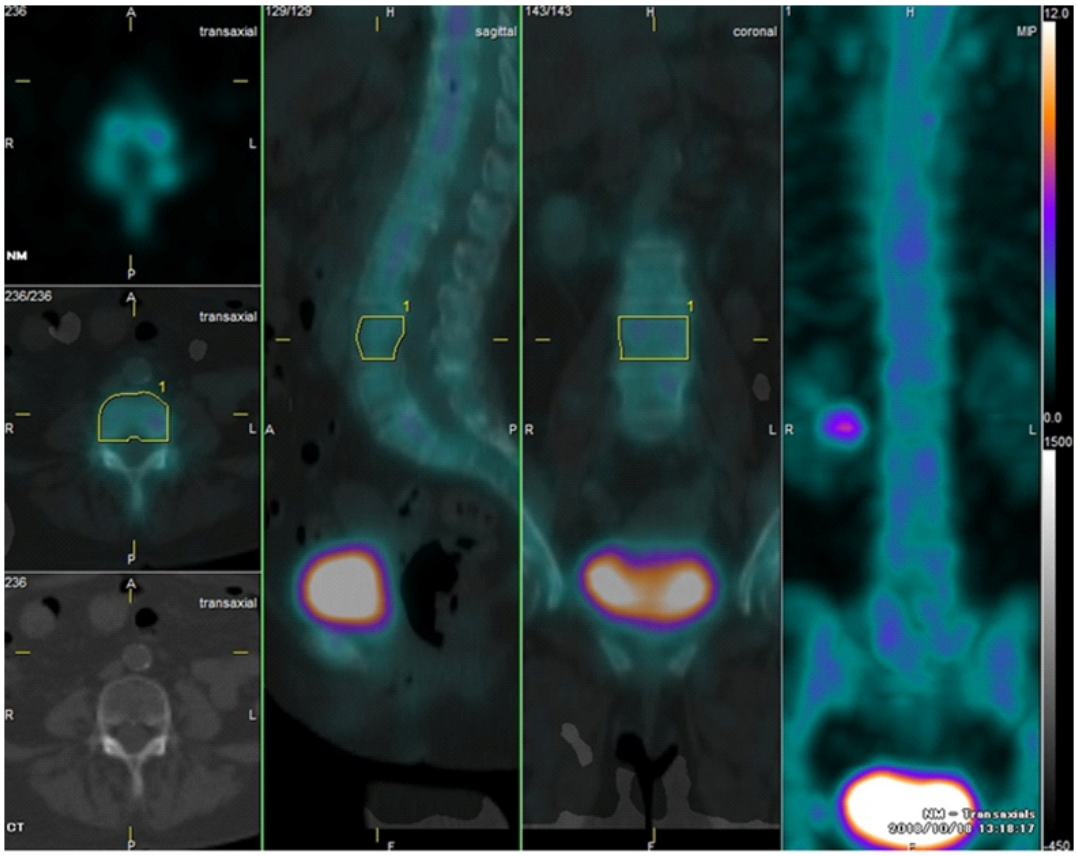

Figure 3. Normal L4 vertebra in a 42-year-old male breast cancer patient, showing a low SUVmax of 4.35.

Statistical analysis

A Shapiro-Wilk normality test was used to analyze data distribution. Values are expressed as average±standard deviation. Differences among the SUVmax of three groups were analyzed using a Kruskal-Wallis test with Dunn's multiple comparisons, while differences between two groups were analyzed using Mann-Whitney's U test. In addition, to determine optimal SUVmax cut-off values offering the best discrimination between two groups, a receiver operating characteristic (ROC) curve was also drawn. SAS, version 9.3 (SAS Institute Inc., Cary, NC, USA), was used to perform statistical analyses, with $P<0.05$ considered to indicate significance.

Results

The mean SUVmax values for the normal L4 bone (n=101), skeletal degenerative changes (n=47), and bone metastasis (n=64) groups were 4.47±1.66 (range 1.01-11.25), 6.99±2.58 (2.21-14.6), and 25.4±15.7 (3.88-98.87), respectively (Figure 4), with a significant difference observed among the three groups ($P<0.001$). Mean SUVmax for the bone metastasis group was significantly greater as compared to that for the normal bone and skeletal degenerative change groups (both $P<0.001$), while no significant difference was noted between the normal bone and skeletal degenerative change groups.

Receiver operating characteristic curves indicated very good diagnostic accuracy for SUVmax to differentiate between bone metastasis and normal bone, with an area under the ROC curve (AUC) value of 0.987. For defining bone metastasis, the optimum SUVmax cut-off value was 7.40. Using that value, we found sensitivity, specificity, and accuracy of 96.3%, 95.1%, and 95.7%, respectively. Also, to discriminate bone metastasis from skeletal degenerative disease, a best discriminative SUVmax cut-off of 11.26 was used based on ROC curve analysis results (AUC 0.933), with sensitivity, specificity, and accuracy of 87.5%, 93.6%, and 90.4%, respectively.

Discussion

The present findings show that discrimination of bone metastasis can be established with high accuracy using SUV parameters. Furthermore, they indicate that skeletal SUVmax may help for differentiation of bone metastasis from skeletal degenerative changes visualized as hot foci, thus increasing bone scintigraphy specificity.

Gamma camera imaging has been traditionally used in nuclear medicine for two-dimensional planar imaging, such as bone scintigraphy with ^{99m}Tc-MDP. Single photon emission

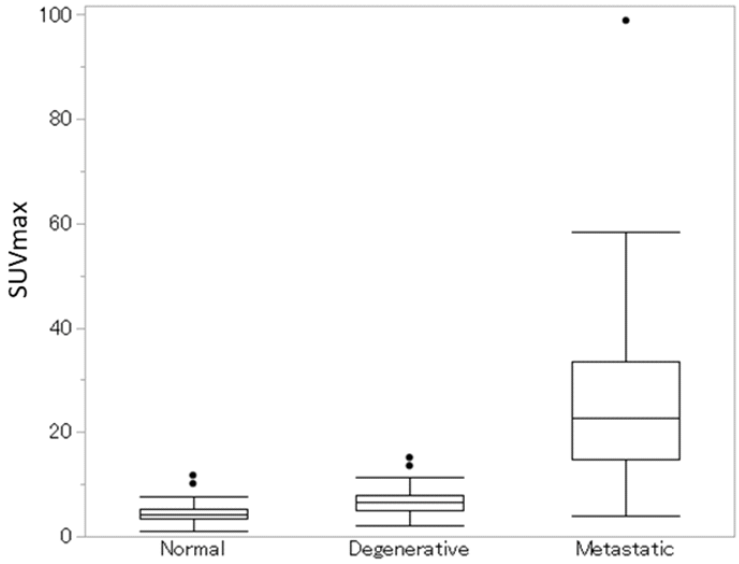

Figure 4. Box-and-whisker plots of SUVmax of the normal bone group, the skeletal degenerative changes group, and the bone metastasis group.

tomography/CT generates imaging voxels, denoted as units of radioactivity per volume (i.e., kBq/mL), by using results of robust algorithms of CT-based three-dimensional attenuation correction, scatter correction, and resolution recovery. That is fundamentally different from planar scintigraphy, SPECT and non-quantitative SPECT/CT, traditional nuclear imaging methods, which utilize counts per second as imaging units. Lesion radioactivity can be normalized for injected radioactivity with quantitative SPECT/CT, thus providing quantitative parameter values, such as percent injected dose and SUV [2-4]. In both phantom (error <3.6%) and patient (error <1.1%) studies, Zeintl et al. (2010) [2] reported that advanced SPECT/CT technology facilitated quantitative ^{99m}Tc SPECT imaging with excellent accuracy. Also, in a phantom study, Gnesin et al. (2016)[4] found that both absolute activity and activity concentration determined with quantitative ^{99m}Tc SPECT/CT were within 10% of expected values.

Following successful clinical application of SPECT/CT findings in patients affected by malignant skeletal disease, quantitative bone SPECT/CT with SUV was developed [5-10]. Using quantitative skeletal SPECT/CT with ^{99m}Tc-diphosphono-propanedicarboxylic acid (^{99m}Tc-DPD), Beck et al. (2016) [5] investigated SUV changes before and after treatment in 16 breast cancer and 3 prostate cancer patients (hormonal therapy and bisphosphonates). Mean SUVpeak and SUVmean values for 52 bone metastasis sites prior to treatment were 20.4±20.8 and 5.6±1.9 respectively, in their study, which decreased after treatment to 16.4±11.5 (19.6% reduction) and 4.9±2.2 (12.5% reduction), respectively. Also, Kitajima et al. (2018) [8] reported a case of periosteal osteosarcoma in which SUVmax values shown by quantitative bone SPECT/CT with ^{99m}Tc-HMDP were useful for evaluating treatment response to preoperative chemotherapy. We consider that quantitative bone SPECT/CT can be very useful for evaluation of treatment response in patients with bone disease. Previously, for monitoring of the efficacy of treatment response in affected patients, scintigraphy without quantitative values was used, though that only provides subjective and ambiguous results. In contrast, quantitative SPECT/CT with SUVmax can provide objective and persuasive findings for accurate evaluation of the efficacy of treatment response. Quantitative SPECT/CT is noninvasive and anticipated to be found useful for accurate treatment response monitoring to determine efficacy in affected patients.

Kuji et al. (2017) [6] evaluated normal vertebral body, skeletal degenerative change and bone metastasis SUV obtained in analyses of 170 prostate cancer patients undergoing bone SPECT/CT with ^{99m}Tc-MDP. Their results showed SUVmax values of 7.58±2.42 for normal thoracic and 8.12±2.24 for normal lumbar vertebral bodies, 16.73±6.74 for skeletal degenerative changes and 40.90±33.46 for bone metastasis. That for the bone metastasis group was significantly greater as compared to the other three groups (P< 0.001). In ROC analyses performed to demonstrate the diagnostic accuracy of SUVmax for discrimination of bone metastasis from skeletal degenerative changes in hot foci, in patient-based mode the area under the ROC curve was 0.840, while that was 0.932 in lesion-based mode. Using quantitative skeletal SPECT/CT with ^{99m}Tc-DPD, Tabotta et al. (2019) [11] analyzed 264 areas of bone metastasis in 26 prostate cancer patients, as well as 24 spinal and pelvic osteoarthritic lesions in 13 patients without cancer and reported a mean SUVmax value of 34.6±24.6 for bone metastasis, as compared to 14.2±3.8 for spinal and pelvic osteoarthritic lesions, with the value for the osteoarthritic group significantly higher (P<0.0001). In another study that used an SUVmax cut-off of 19.5 for prostate cancer bone metastases in the spine and pelvis, sensitivity and specificity were 87% and 92%, respectively. The results of these reports are very similar to those obtained in the present series.

Other investigations have shown a wide range of values for normal vertebral SUV. Kaneta et al. (2016) [12] determined

SUV in 29 patients with normal Th4-L4 vertebrae findings obtained with ^{99m}Tc-MDP bone imaging and reported an SUVmax value of 7.1±1.5 for 189 vertebral images. Also, Cachovan et al. (2013) [13] analyzed a total of 145 normal lumbar spine images (L3-L5) of 50 female subjects obtained with ^{99m}Tc-DPD bone imaging and reported an SUVmean value of 5.91±1.54. In a study presented by Umeda et al. (2018) [7], mean SUVmax values for normal Th12 and S3 shown by ^{99m}Tc-MDP bone imaging of 69 patients were 5.71±1.37 and 5.32±1.4, respectively, similar to the present findings, while Huang et al. (2020) [14] noted SUVmax and SUVmean values for normal L1-L4 vertebrae in 62 patients who underwent ^{99m}Tc-MDP bone imaging of 7.39±1.84 and 4.90±1.27, respectively. However, because different research institutes use a variety of instruments as well as differences in acquisition parameters, reconstruction algorithms, correction technology, radiopharmaceutical factors and measurement location, research results are not directly comparable. It is considered extremely important to establish a unified standard procedure for quantification of SPECT/CT results, while the gold standard of SUV for normal bone tissue in different areas should be further clarified.

Other nuclear medicine modalities are available for detection and characterization of bone metastasis, especially for prostate cancer patient examinations. Positron emission tomography protocols using prostate specific membrane antigen (PSMA), choline, and sodium fluoride (NaF) have been shown to have very good accuracy for diagnosis of prostate cancer bone metastasis [15-17], with the most promising modality possibly PSMA PET. However, PSMA, choline and NaF are not widely available in many countries for primary staging or restaging, due to cost and reimbursement issues and the impact on patient management is not known and cost-effective studies have yet to be published. An investigation that compared prostate specific antigen (PSA) cut-off values for ordering fluorine-18 (^{18}F)-NaF PET or bone scintigraphy for examinations of patients with newly diagnosed prostate cancer showed no major difference between those modalities [18]. Also, a recent study of patients with prostate and breast cancer by Arvola et al. (2019) [19] reported a strong correlation between SUV obtained with ^{99m}Tc-HDP SPECT/CT and ^{18}F-NaF PET/CT. The authors concluded that SPECT is applicable for clinical quantification of bone metabolism in osseous metastasis areas in breast and prostate cancer patients. Therefore, use of quantitative bone scintigraphy seems to increase the accuracy of bone SPECT/CT, allowing that to remain competitive in this era of new multimodality imaging of bone metastasis associated with prostate cancer.

This study has some limitations, including the small subject population. In addition, histological confirmation for all bone metastases, skeletal degenerative changes and normal bone is lacking.

In conclusion, the present results show that discrimination of bone metastasis high accuracy can be obtained based on SUV derived from three-dimensional quantitative bone SPECT/CT. Hence, additional quantitative data analysis to bone scan interpretation can help to more confidently distinguish metastatic from benign focal bone lesions, thus increasing the overall diagnostic performance of bone scintigraphy. Additional studies that examine greater numbers of patients will be necessary to define its impact for clinical evaluations, diagnosis of bone metastasis and assessing treatment response.

The authors declare that they have no conflicts of interest.

Funding Source
This study was supported by a Grant-in-Aid from the Ministry of Education, Culture, Sports, Science, and Technology of Japan (No. 22K07757).

Bibliography

1. Helyar V, Mohan HK, Barwick T et al. The added value of multislice SPECT/CT in patients with equivocal bony metastasis from carcinoma of the prostate. *Eur J Nucl Med Mol Imaging* 2010; 37: 706-13.
2. Zeintl J, Vija AH, Yahil A et al .Quantitative accuracy of clinical ^{99m}Tc SPECT/CT using ordered-subset expectation maximization with 3-dimensional resolution recovery, attenuation, and scatter correction. *J Nucl Med* 2010; 51: 921-8.
3. Bailey DL, Willowson KP. An evidence-based review of quantitative SPECT imaging and potential clinical applications. *J Nucl Med* 2013; 54: 83-9.
4. Gnesin S, Leite Ferreira P et al. Phantom validation of ^{99m}Tc absolute quantification in a SPECT/CT commercial device. *Comput Math Methods Med* 2016; 2016: 4360371.
5. Beck M, Sanders JC, Ritt P et al. Longitudinal analysis of bone metabolism using SPECT/CT and ^{99m}Tc-diphosphono-propanedicarboxylic acid: comparison of visual and quantitative analysis. *EJNMMI Res* 2016; 6: 60.
6. Kuji I, Yamane T, Seto A et al. Skeletal standardized uptake values obtained by quantitative SPECT/CT as an osteoblastic biomarker for the discrimination of active bone metastasis in prostate cancer. *Eur J Hybrid Imaging* 2017; 1: 2.
7. Umeda T, Koizumi M, Fukai S et al. Evaluation of bone metastatic burden by bone SPECT/CT in metastatic prostate cancer patients: defining threshold value for total bone uptake and assessment in radium-223 treated patients. *Ann Nucl Med* 2018; 32: 105-13.
8. Kitajima K, Futani H, Fujiwara M et al. Usefulness of quantitative bone single photon emission computed tomography/computed tomography for evaluating response to neoadjuvant chemotherapy in a patient with periosteal osteosarcoma. *Cureus* 2018; 10: e3655.
9. Kitajima K, Futani H, Tsuchitani T et al. Quantitative bone SPECT/CT applications for cartilaginous bone neoplasms. *Hell J Nucl Med* 2020; 23: 133-7.
10. Kitajima K, Futani H, Komoto H et al. Quantitative bone SPECT/CT applications for primary bone neoplasms. *Hell J Nucl Med* 2021; 24: 36-44.
11. Tabotta F, Jreige M, Schaefer N et al. Quantitative bone SPECT/CT: high specificity for identification of prostate cancer bone metastases. *BMC Musculoskelet Disord* 2019; 20: 619.
12. Kaneta T, Ogawa M, Daisaki H et al. SUV measurement of normal vertebrae using SPECT/CT with ^{99m}Tc methylene diphosphonate. *Am J Nucl Med Mol Imaging* 2016; 6: 262-8.
13. Cachovan M, Vija AH, Hornegger J, Kuwert T. Quantifcation of ^{99m}Tc-DPD concentration in the lumbar spine with SPECT/CT. *EJNMMI Res* 2013; 3: 1-8
14. Huang K, Feng Y, Liu D et al. Quantification evaluation of ^{99m}Tc-MDP concentration in the lumbar spine with SPECT/CT: compare with bone mineral density. *Ann Nucl Med* 2020; 34: 136-43.
15. Even-Sapir E, Metser U, Mishani E et al. The detection of bone metastases in patients with highrisk prostate cancer: ^{99m}Tc-MDP planar bone scintigraphy, single- and multi-field-of-view SPECT, ^{18}F-fluoride PET, and ^{18}F-fluoride PET/CT. *J Nucl Med* 2006; 47: 287-97.

16. Pyka T, Okamoto S, Dahlbender M et al. Comparison of bone scintigraphy and ^{68}Ga-PSMA PET for skeletal staging in prostate cancer. *Eur J Nucl Med Mol Imaging* 2016; 43: 2114-21.
17. Kitajima K, Fukushima K, Yamamoto S et al. Diagnostic performance of ^{11}C-choline PET/CT and bone scintigraphy in the detection of bone metastases in patients with prostate cancer. *Nagoya J Med Sci* 2017; 79: 387-99.
18. Cook GJ, Azad G, Padhani AR. Bone imaging in prostate cancer: the evolving roles of nuclear medicine and radiology. *Clin Transl Imaging* 2016; 4: 439-47.
19. Arvola S, Jambor I, Kuisma A et al. Comparison of standardized uptake values between ^{99m}Tc-HDP SPECT/CT and ^{18}F-NaF PET/CT in bone metastases of breast and prostate cancer. *EJNMMI Res* 2019; 9: 6.